OXIDATIVE METABOLISM OF THE TRIFLUOROMETHOXY MOIETY OF OSI-930

Larry Dihel[1], Christine Kittleson[2], Kristen Mulvihill[2] and William W. Johnson[1]*

[1]*Drug Metabolism and Pharmacokinetics, OSI Pharmaceuticals, Inc., Boulder, CO and*
[2]*Chemical Operations, OSI Pharmaceuticals, Farmingdale, NY, USA*

SUMMARY

Cytochrome P450 can catalyze a wide array of remarkable oxidations, including *O*-dealkylations, which are performed via oxidation of the α-carbon of the ether. When C-H bonds are replaced with C-F bonds, however, the bond strength is much greater, and it significantly deters oxidation at the carbon. Another recently elucidated reaction catalyzed by P450, *ipso* substitution, results in displacement of aromatic ring substituents such as an alkoxy group via hydroxyl substitution. Through LC/MS/MS, we show the CYP-mediated oxidative displacement of the trifluoromethoxy group from the phenyl constituent in OSI-930, a novel small molecule c-Kit/VEGF-r inhibitor in clinical studies to treat cancer. Based on C-F bond strength, reported phenacetin studies, and α-quaternary alkylphenol studies, we propose an *ipso*-substitution mechanism for this oxidative biotransformation. *In vivo*, this hydroxylated metabolite goes on to form the ether conjugate with glucuronide.

KEY WORDS

P450, *ipso* substitution, trifluoromethoxy, oxidation biotransformation

* Author for correspondence:
William W. Johnson
Drug Metabolism and Pharmacokinetics
OSI Pharmaceuticals, Inc.
2860 Wilderness Place
Boulder, CO 80301, USA
e-mail: bjohnson@osip.com

INTRODUCTION

Cytochrome P450 monooxygenases catalyze diverse oxidations including hydroxylation of aliphatic and aromatic carbons, epoxidations of olefins, *N*-dealkylation of amines, and *O*-dealkylation of ethers by activation of molecular oxygen /1,2/. Many drugs are metabolized by cytochrome P450 catalyzed oxidation to result generally in more hydrophilic and, hence, expellable compounds. CYP-mediated oxidation of alkoxy xenobiotics (aromatic ethers) generally results in *O*-dealkylation from a hemiacetal intermediate via oxidation of the α-carbon of the ether, as illustrated in Figure 1 /3-5/. The initial step in the activation of substrates by cytochrome P450 is either one-electron oxidation (abstraction of an electron) or hydrogen abstraction (abstraction of an electron and a proton). After the initial one-electron step, the oxidized substrate can either recombine with the activated oxygen species to yield oxygenated products or undergo a second one-electron step leading to hydrogen abstraction. *O*-Dealkylation reactions are mediated by direct insertion of the oxygen into the vicinal C-H bond, as electron abstraction from the oxygen is too difficult due to its high oxidation potential relative to nitrogen or sulfur heteroatoms, then the resulting hemiacetal breaks down to the corresponding phenol and aldehyde (Fig. 1).

Incorporation of a fluorine substituent in drug molecules has been widely exploited to abrogate biotransformation /6,7/. The ease of halogen elimination in cytochrome P450-catalyzed oxidative dehalogenation decreases in the order F > Cl > Br > I /8/. Fluorine, the most electronegative element in the periodic table, forms a very strong bond with carbon (C-F bond energy = 116 kcal/mol) as compared with the carbon-hydrogen bond (C-H bond energy = 99 kcal/mol). Consequently, the introduction of fluorine can block hydroxylation or enhance metabolic stability at the modified position /9/. CYP-mediated defluorination of the fluoromethyl group is extremely rare, although 5-trifluoromethyluracil is converted to 5-carboxyuracil with the release of fluoride /10/, and the presence of a *p*-hydroxyl group can lead to spontaneous decomposition to a carboxylic acid formed from an intermediate quinone methide /11/. Oxidative C-F bond scission in a trifluoromethoxy group is very different from the above examples, however, and has only recently been demonstrated for a system with a methoxy in the *para* position, CP-122,721 /12/, as shown in Figure 2.

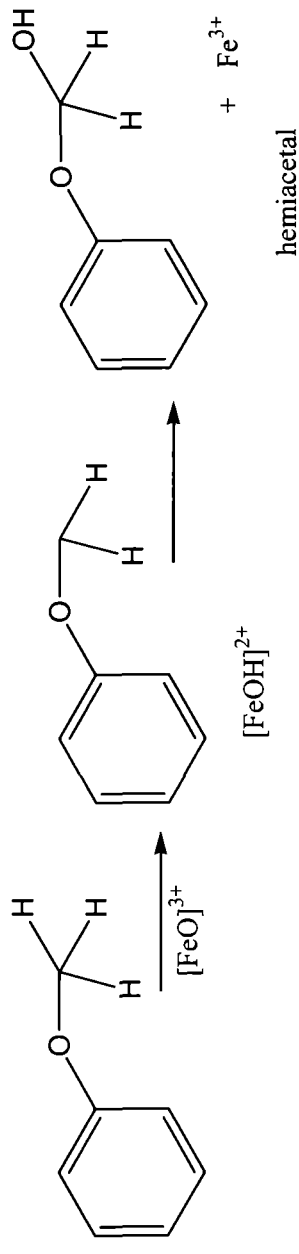

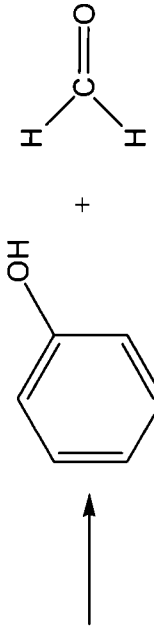

O-demethylation, general scheme

Fig. 1: Canonical *O*-demethylation scheme.

In the course of investigating the biotransformation of OSI-930 we isolated and characterized various P450-mediated metabolites. Among the various plausible metabolites of OSI-930 *in vivo* and *in vitro* we have observed the unexpected loss of the trifluoromethoxy group which is *para* to an aminoacyl moiety and the cytochrome P450-mediated metabolism is thought to involve *ipso* substitution. The objective of this report is a description of this *des*-trifluoromethoxy OSI-930 metabolite and support for an *ipso*-substitution mechanism.

MATERIALS AND METHODS

In vitro and time-based intensity analysis

HPLC was carried out by an Agilent 1100 pump and degasser system coupled to a Leap CTC Pal auto-sampler. A gradient HPLC method was developed using 10 mM ammonium formate in water (A) and 10 mM ammonium formate in 10% water/90% methanol (B). The initial starting conditions ran for 10 minutes at 50% B and then increased linearly for 25 minutes to 100% B and held for 9 minutes. The %B was then linearly decreased for 1 minute to the starting conditions and held for 5 minutes with a total method run time of 45 minutes. The gradient was applied to a Phenomenex® Gemini™ C6-phenyl 2.0 x 150 mm, 5µ column with a corresponding guard column at 250 µl/minute.

Plasma from rats given a single oral dose of OSI-930 (3-[(quinolin-4-ylmethyl)amino]-*N*-[4-(trifluoromethox)phenyl]thiophene-2-carboxamide) at 1000 mg/kg was used to identify the de-trifluoromethoxy (dTFM) metabolite and also for the time-course study. Nominal time points were 0.5, 1, 2, 4, 8, 12, 24 and 48 hours. The OSI-930 C_{max} was 11 µM. An aliquot of plasma (200 µl) was diluted with methanol (200 µl), vortexed, and then centrifuged at 14,000 *g* for approximately 10 minutes. The clear supernatant was transferred to a clean HPLC vial for analysis. The injection volume was set at 20 µl.

Pooled human liver microsomes, purchased from In Vitro Technologies, Inc., Baltimore, MD, USA, were supplemented with appropriate cytochrome P450 co-factors such as NADPH. Incubations were conducted at 37°C for 60 minutes. Final reaction mixtures contained 1 mg/ml human liver microsomal protein, 2 mM NADPH, 5 µM test compound (comparable to systemic *in vivo* exposures in the

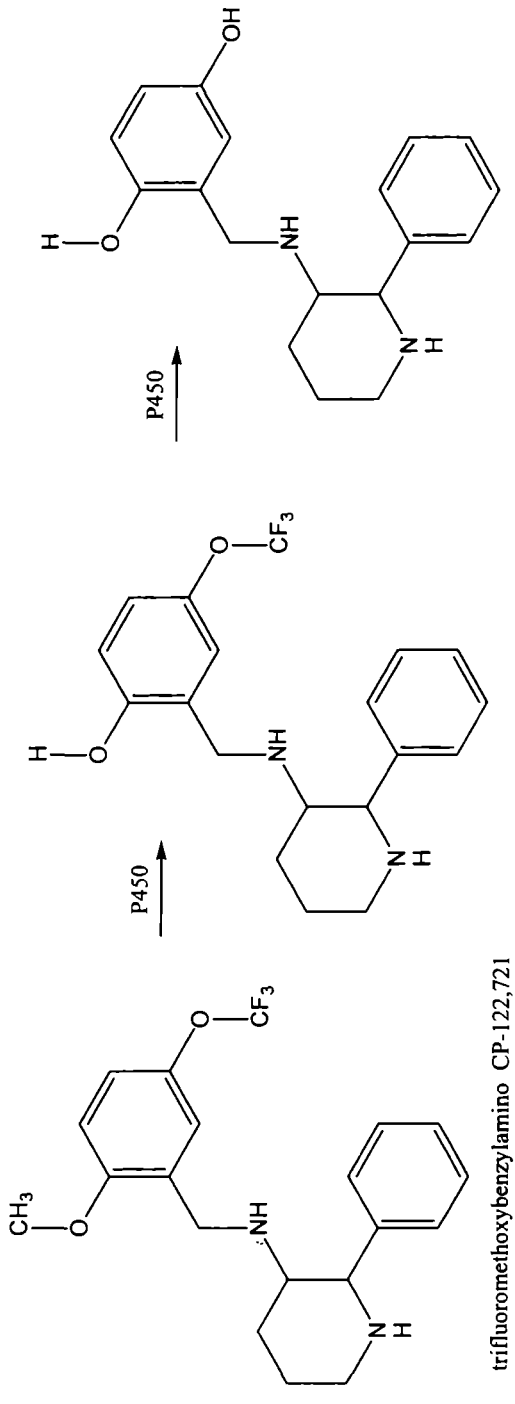

Fig. 2: Biotransformation product of trifluoromethoxybenzylamino CP-122,721.

high-dose rats, C_{max} was about 11 μM). Control assays with no NADPH and no test compound were performed. Incubation reaction mixtures were brought to a final volume of 300 μl with the addition of 50 mM potassium phosphate buffer (pH 7.4). Acetonitrile (0.6 ml) was used to terminate incubations. Reaction mixtures were centrifuged for 15 min at 17,000 *g*. Supernatants were then transferred to another tube and stored at -20°C until analysis.

Recombinant cytochrome P450 incubations

The individually expressed cytochrome P450s were purchased from Xeno Tech, LLC Lenexa, Kansas. The relative purities of cytochromes P450 2D6, P450 3A4, P450 2A6, and P450 2B6 were 6.4, 8.5, 3.0, and 1.5 nmol/ml at a total protein amount of 10 mg/ml. Conditions were equivalent to the microsomal incubations except for the following: final reaction mixtures contained 1 mM NADPH, and P450 concentrations varied from 8-13 pmol/ml with OSI-930 concentration at 9.95 μM and incubation at 37°C for 20 minutes. Samples were prepared similarly to the plasma sample method, i.e., stopped and precipitated with the addition of two volumes of methanol. Testosterone was used as a positive control.

LC-MS/MS

Supernatant (200 μl) was transferred to a 96-well plate and evaporated to dryness under a nitrogen stream at 35°C. Samples were resuspended in 100 μl water/methanol, 95%/5% v/v, matching the initial chromatographic conditions.

A Sciex® API 4000QTrap mass spectrometer (MDS Sciex, Concord, Ontario, Canada) with a Q3 region that is convertible from a quadrupole to a linear ion trap (LIT) was used for all experiments. The standard quadrupole function of the Q3 region allows for standard multi-reaction monitoring (SRM), neutral loss (NL), and product ion (PrI) and precursor ion (PI) scan modes that can be used to identify the parent drug and reveal metabolites using MS/MS. The conversion of Q3 from the quadrupole to the LIT function can be triggered on a millisecond time scale using an information-dependent acquisition (IDA) script to give high resolution product ion spectra. Also, the LIT function in conjunction with Q1 MS and Q2 collision induced disassociation (CID) and further fragmentation in the LIT allowed for

high resolution MS/MS/MS (MS^3) experiments to identify secondary product ions.

Source and analyte conditions were optimized by infusion of a 10 ng/ml solution of OSI-930 in 10 mM formic acid in 50% water/50% methanol at a flow of 10 µl/min. For all experiments, source conditions were set at values of 5500 V for the ionization energy setting and 400°C for temperature setting, a setting of 30 for curtain gas, and settings of 40 and 70 for gas 1 and 2, respectively. Analyte conditions were set at 30 V for the declustering potential and 10 V for the exit potential. Collision gas was set at high, while collision energy was set at 35 eV. For SRM data, Q1 and Q3 resolution were set at unit and low resolution, respectively. For product ion spectra, Q1 was set at low, and the LIT fill time was set on DYNAMIC (an automated optimization setting) with a scan rate of 4000 amu/sec.

Data were analyzed using Analyst 1.4.1 Metabolism ID software and by visual inspection using Analyst 1.4.1 software graphics (Applera Corporation, Applied Biosystems, Foster City, CA).

Spectral data

Plasma from rats given a single oral dose of OSI-930 at 500 mg/kg was used for the generation of product ion spectra. Aliquots of 50 µl from four individual animals at a 24 hour time point were pooled. This pooled sample (200 µl) was added to ethyl acetate (400 µl), mixed for approximately 10 minutes and then centrifuged at 14,000 *g* for approximately 10 minutes. The cleared supernatant was transferred to a clean HPLC vial for analysis. Authentic dTFM (OSIP691251) was added to blank rat plasma at an approximate concentration of 100 pg/ml. Sample extraction was identical to pooled samples. The injection volume for all samples was set at 20 µl. The HPLC method described above was changed to 0.1% formic acid in water (A) and 0.1% formic acid in 10% water/90% methanol (B). The initial starting conditions ran for 10 minutes at a ratio of 55:45 A to B. Then the gradient was increased linearly for 25 minutes to a ratio of 0:100 and held for 9 minutes. The gradient was then linearly decreased for 1 minute to the starting conditions and held for 5 minutes. The total method run time was 45 minutes.

MS spectrum of synthetic standard

Source and analyte conditions were optimized by infusion of a 10 ng/ml solution of OSI-930 in 10 mM formic acid in 50% water, 50% methanol at a flow rate of 10 µl/min. For all experiments source conditions were set at values of 5500 V for the ionization energy setting and 400°C for temperature setting, a setting of 30 for curtain gas, and settings of 40 and 70 for gas 1 and 2, respectively. Analyte conditions were set at 30 V for the declustering potential, 10 V for the exit potential. Collision gas was set at high and collisions energy was set at 35 eV. For SRM data resolution for Q1 and Q3 were set at unit and low resolution, respectively. For product ion spectra Q1 was set at low and the LIT fill time was set on DYNAMIC (an automated optimization setting) with a scan rate of 4000 amu/sec. Data were analyzed using Analyst 1.4.1 Metabolism ID software and by visual inspection using Analyst 1.4.1 software graphics (Applera Corporation, Applied Biosystems, Foster City, CA).

Synthesis of *N*-(4-hydroxyphenyl)-3-[(quinolin-4-ylmethyl)amino] thiophene-2-carboxamide

Commercially available reagents, anhydrous solvents, and HPLC-grade solvents were used without further purification. Flash chromatography was performed over silica gel (400-230 mesh). Mass-directed purification was performed on a Waters system composed of the following: 2767 Sample Manager, 2525 Binary Gradient Module, 600 Controller, 2487 Dual λ Absorbance Detector, Micromass ZQ for mass ionization, Phenomenex Luna 5µ C18(2) 100 Å 150 x 21.2 mm 5µ column with mobile phases of 0.01% formic acid acetonitrile (A) and 0.01% formic acid in HPLC water (B). The flow rate was 20 ml/min, run time of 13 min, and a gradient profile of 0.00 min 2%A, 2.10 min 10%A, 8.00 min 50%A, 12.0 min 99%A, 12.8 min 2%A. LC-MS data were collected on either OpenLynx or ZQ3. OpenLynx is an Agilent 1100 HPLC equipped with a Gilson Auto injector and Waters Micromass ZQ for ionization. The column used was an Xterra MS C18, 5µ particle size, 4.6 × 50 mm with a mobile phase of acetonitrile (A) and 0.01% formic acid in HPLC water (B). The flow rate was 1.3 ml/min, run time of 5 min, and a gradient profile of 0.00 min 5%A, 3.00 min 90%A, 3.50 min 90%A, 4.00 min 5%A, 5.00 min 5%A. ^{1}H-NMR (400 MHz) and ^{13}C-NMR (100.6 MHz) spectra were

recorded at ambient temperature with TMS or the residual solvent peak as the internal standard. The line positions or multiples are given in ppm (δ), and the coupling constants (*J*) are given as absolute values in Hertz (Hz). High resolution mass spectral analysis (HRMS) was obtained by M-Scan Inc., West Chester, PA.

A solution of 4-aminophenol (122 mg, 1.12 mmol) in anhydrous toluene (2.7 ml) was treated drop-wise with 2.0 M trimethylaluminum in toluene (1.46 ml, 2.90 mmol) at room temperature (rt). The mixture was then heated at 70°C for 2 h. Methyl 3-[(quinolin-4-ylmethyl) amino]thiophene-2-carboxylate[1] (**1**, 0.300 g, 1.00 mmol) was added in one portion and the mixture heated at 70°C for 2 h. The reaction was then cooled to rt, and after being stirred for 72 h, the reaction was poured into saturated $NaHCO_3$ (20 ml) and extracted with EtOAc (3 × 20 ml). The combined organics were washed with water and brine, and dried over $MgSO_4$. The suspension was filtered and concentrated *in vacuo* to afford title compound **2** as an off-white solid (140 mg, 34% yield) (Fig. 3). A sample was further purified using mass-directed purification to provide the title compound **2** as an off-white solid. ^{1}H-NMR (400 MHz, DMSO): δ 5.05 (d, *J* = 5.6 Hz, 2H), 6.70 (ddd, *J* = 10.0, 3.2, 3.2 Hz, 2H), 6.79 (d, *J* = 5.6 Hz, 1H), 7.37-7.42 (m, 3H), 7.54 (d, *J* = 5.6 Hz, 1H), 7.66 (ddd, *J* = 8.0, 6.8, 0.8 Hz, 1H), 7.79 (ddd, *J* = 8.0, 6.8, 1.2 Hz, 1H), 8.02 (dd, *J* = 6.8, 6.8 Hz, 1H), 8.06 (d, *J* = 8.0 Hz, 1H), 8.22 (d, *J* = 8.0 Hz, 1H), 8.83 (d, *J* = 4.8 Hz 1H), 9.18 (s, 1H). ^{13}C-NMR (100 MHz, DMSO): δ 44.9, 101.5, 114.8, 117.6, 118.7, 123.0, 123.2, 123.6, 126.0, 126.6, 129.3, 129.4, 129.6, 130.3, 145.5, 147.6, 150.4, 153.6, 163.3. MS (ES+): *m/z* 376 (M^++H). HRMS *m/z* calculated for $C_{21}H_{17}N_3O_2S$ 376.1120, found 376.1115.

Glucuronide hydrolysis

A solution of β-glucuronidase was prepared by adding 5 mg β-glucuronidase at 10,400 U/mg to 500 µl of phosphate buffered saline to make a 10 mg/ml stock. Plasma from Sprague-Dawley rats given a single oral dose of OSI-930 was pooled. 100 µl of rat plasma with the addition of 30 µl of PBS was mixed and set aside at 4°C; an identical sample was prepared and incubated at 37°C overnight (approximately 14 hours) along with 100 µl plasma sample with the addition of 30 µl

[1] Synthesis of **1** can be found in: Wynne G, Doyle K, Ahmed S, Li An-Hu, et al. (2-Carboxamido)(3-amino)thiophene compounds. US6949563B2

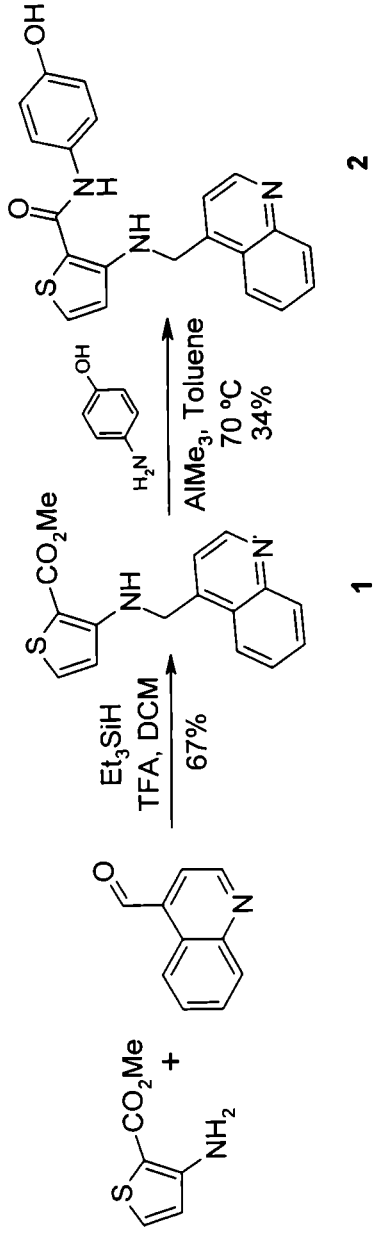

Fig. 3: Synthetic route and method.

of PBS containing β-glucuronidase. The above samples were extracted with an equal volume of 0.1% formic acid in methanol. Extracted samples were analyzed by LC/MS/MS.

RESULTS

Liquid chromatography tandem quadrupole mass spectrometry (LC/MS/MS) positive ion constant neutral loss (NL) scanning at a differential of 176 *u* (unified atomic mass unit) revealed a unique and substantial metabolite peak with a molecular ion at 552 *m/z* in the plasma of Sprague-Dawley rats given a single oral dose of OSI-930 (Fig. 4). The enhanced product ion spectrum of this peak suggested a possible molecular structure that was consistent with the loss of the trifluoromethyl group followed by conjugation with glucuronide at the newly exposed hydroxyl group. The neutral loss of 176 *u* is characteristic of a glucuronide conjugate. Various predictable OSI-930 metabolites were characterized by LC/MS/MS, and several structures were confirmed by synthetic reference standards. These results provided consistent characteristic fragment ion peaks important for structural assignments. One such metabolite showed a molecular ion at 552 *m/z* with distinguishing product ions at 376 and 267 *m/z* that are known to be representative of the *des*-trifluoromethyl (dTFM) and thiophene-containing molecular substructures (Fig. 4). The peaks at 267 and 239 *m/z* represent product ions of the quinoline thiophene compound with or without the carbonyl, respectively, as shown in the figure insert. The enhanced product ion spectrum (EPI) of the novel OSI-930 *des*-trifluoromethyl + glucuronide (dTFM + glucuronide) metabolite extracted from rat plasma is shown in Figure 4. The EPI spectrum has a molecular ion at *m/z* 552 and a novel product ion at *m/z* 376. Characteristic ions in common with OSI-930 are shown at 267, 249, 239, 234, 143, 130, and 126 *m/z*.

The identification of the 552/376 *m/z des*-trifluoromethyl-glucuronide metabolite indicated that a *des*-trifluoromethyl intermediate (dTFM) transformation product should also be present in the plasma of rats given OSI-930. This intermediate molecule should be missing the trifluoromethyl group for a net loss of 68 *u* (relative to OSI-930 parent molecule at *m/z* 444), yielding a molecular ion at 376 *m/z*, and should have product ions characteristic of OSI-930. The molecular structures are shown in Figure 5. A dTFM molecule was then

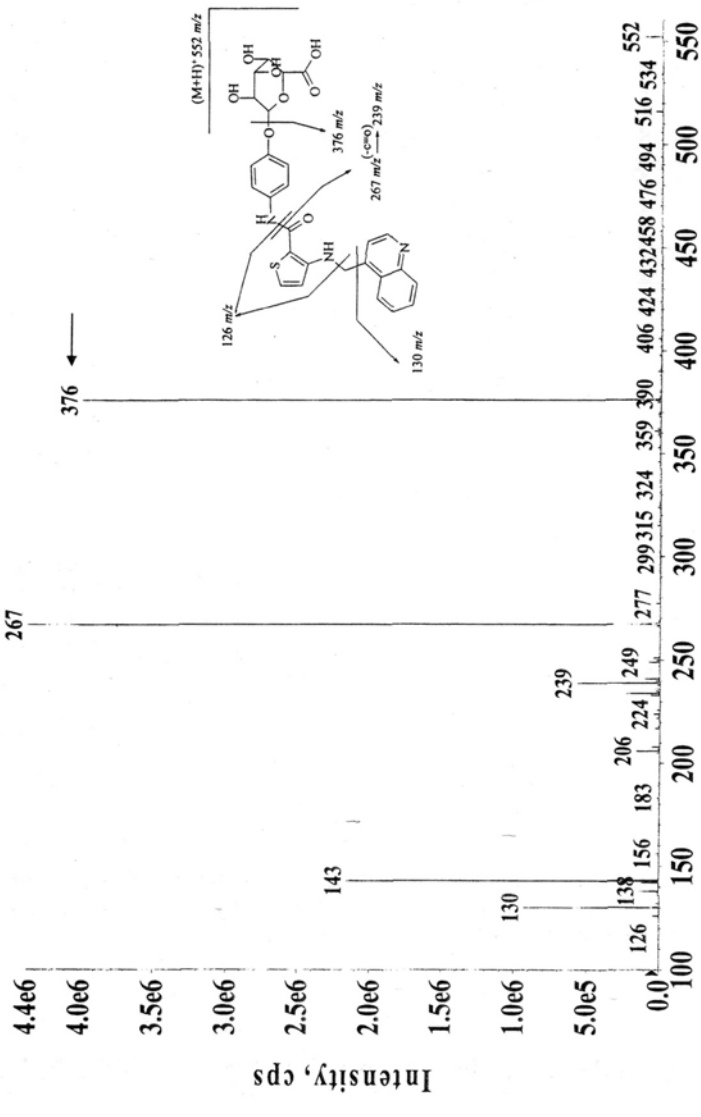

Fig. 4: Enhanced product ion spectra of OSI-930-*des*-trifluoromethyl + glucuronide (dTFM + glucuronide, 552/376 *m/z*). A unique ion at an *m/z* of 376 is noted with an arrow. The x-axis is in *m/z* and the y-axis is percent relative intensity.

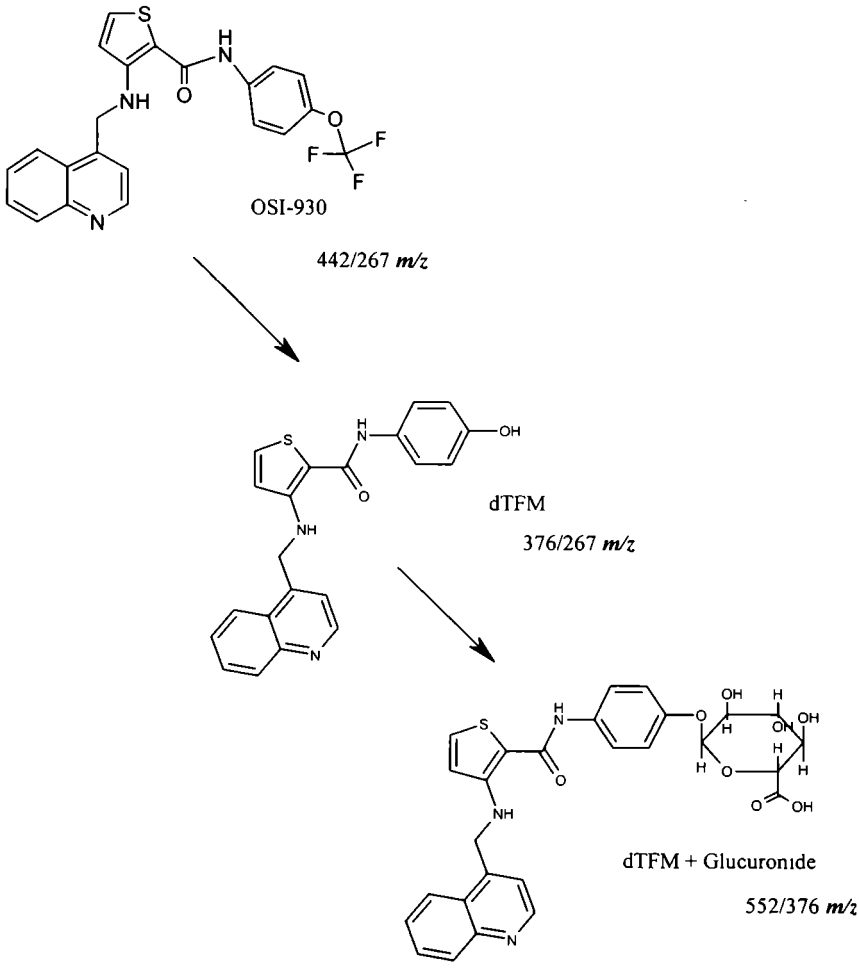

Fig. 5: Schematic of the proposed intermediate metabolite, OSI-930 *des*-trifluoromethyl (dTFM) and OSI-930 *des*-trifluoromethyl + glucuronide (dTMF + glucuronide). Mass to charge (*m/z*) transitions are shown.

chemically synthesized, identical to OSI-930 except that a hydroxyl group was substituted in place of the trifluoromethoxy group. This molecule, OSIP691251, was characterized by infusion at 100 ng/ml into the ABI4000QTrap. A high-resolution enhanced product ion spectrum is shown in Figure 6, with product ion assignments shown in

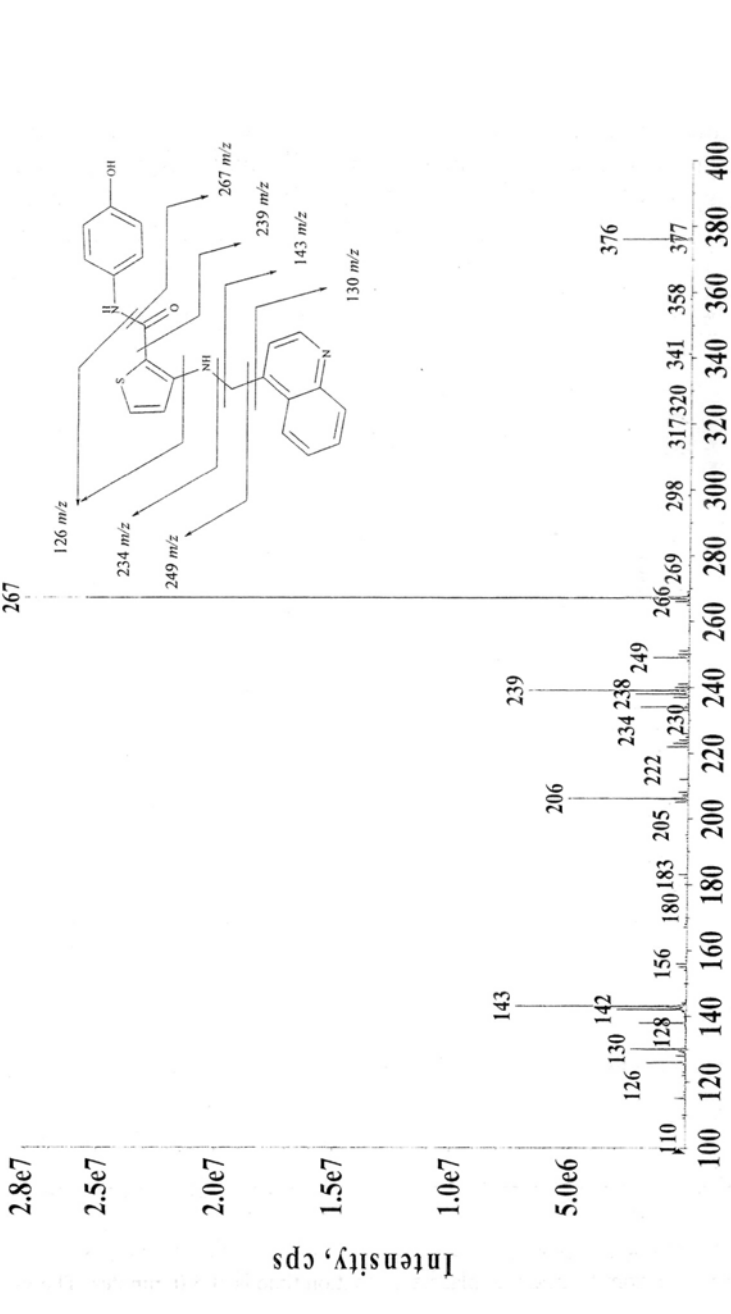

Fig. 6: OSI-930 *des*-trifluoromethyl synthetic compound enhanced product ion data were gathered via infusion of a 100 ng/ml stock of OSIP691251, in 0.1% formic acid:50% water:50% methanol. The molecular ion, $(M+H)^+$, is shown at 376 *m/z*. Rational product ion assignments to molecular structure are given in the interior diagram. Characteristic ions are shown at 267, 249, 239, 234, 143, 130, and 126. The x-axis is in *m/z* and the y-axis is intensity in counts per second (cps).

the insert. Note that ions at 376, 267, 249, 239, 234, 143, 130, and 126 *m/z* are also present in the enhanced product ion spectrum of the dTFM + glucuronide metabolite shown in Figure 4. When mixed with blank rat plasma, extracted, separated by HPLC, and analyzed by mass spectrometry, OSIP691251 shows an XIC peak at an *m/z* transition of 376/267 and at a retention time of 5.0 minutes (Fig. 7). At this time,

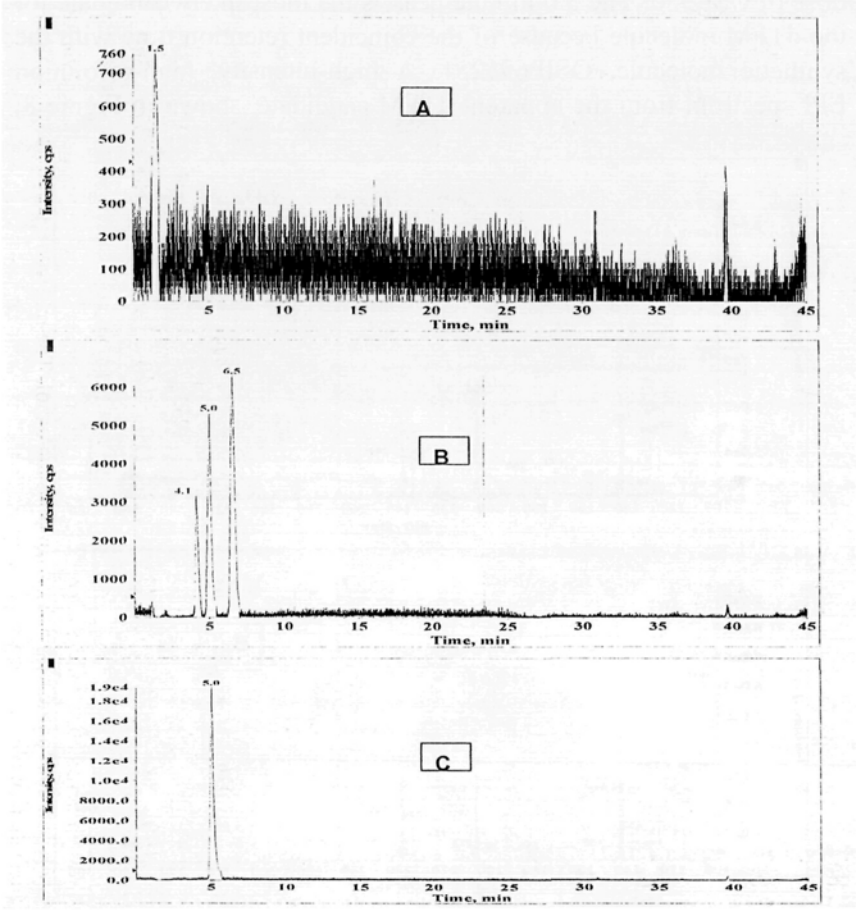

Fig. 7: XIC retention time peak of the synthetic dTFM molecule, OSIP691251, extracted from fortified rat plasma. Retention time is at 5.0 minutes. The x-axis is in *m/z* and the y-axis is intensity in counts per second (cps). **A:** XIC of 376/267 *m/z* from blank rat plasma. **B:** XIC of 376/267 *m/z* from plasma of rats given a single oral dose of OSI-930. **C:** XIC of 376/267 *m/z* blank rat plasma fortified with authentic/synthetic OSIP691251.

however, the XIC peaks at 4.1 and 6.5 cannot be ruled out since a precursor ion survey did not find potential precursor ions for the peaks at 4.1 and 6.5 minutes. The compound at 4.1 minutes is likely a regio-isomer.

A search was initiated for the inferred intermediate dTMF metabolite in rat plasma. Spectral results are shown in Figure 7. Panel A shows the spectrum of the 376/276 *m/z* from rats given a single oral dose of OSI-930. The 5.0 minute peak is the most likely candidate for the dTFM molecule because of the coincident retention time with the synthetic molecule, OSIP691251. A high-intensity, high-resolution EPI spectrum from the apparent dTFM candidate, shown in Figure 8,

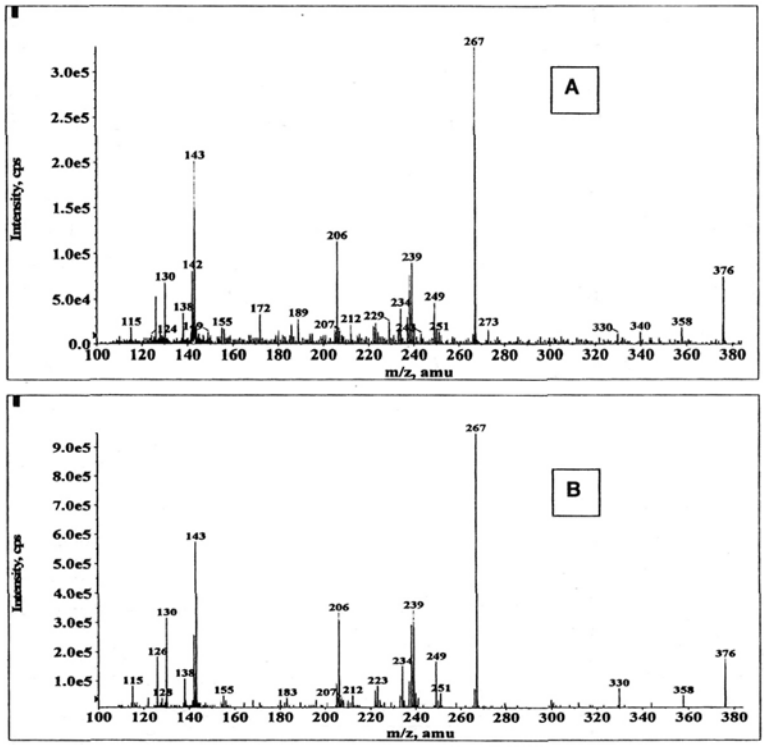

Fig. 8: **A:** Enhanced product ion spectrum derived from the 5 minute HPLC putative dTFM retention time peak from the plasma of rats given a single oral dose of OSI-930. **B:** Enhanced product ion spectrum derived from the 5 minute HPLC retention time peak from authentic dTFM reconstituted into blank rat plasma and extracted. Product ions at 267, 249, 239, 234, 143, 130 and 126 m/z are shown in both figures and are characteristic of the spectra of OSI-930 and infused OSIP691251.

has a remarkable quantity of product ions (≥7) in common with the spectrum of OSIP691251. Both spectra show a molecular ion at *m/z* 376 and product ions in common at 267, 249, 239, 234, 143, 130, and 126 *m/z*. The EPI spectrum of the dTFM metabolite and the synthetic standard show these characteristic peaks represented in the previously illustrated substructures.

With the addition of the hydrolysis enzyme β-glucuronidase to the purported conjugate, the aglycone can be liberated. This reaction can therefore confirm a glucuronide conjugate as a substrate thus characterizing this precursor. This experiment was performed on the plasma samples from an *in vivo* study in which the animals had adequate exposure to OSI-930. Plasma of Sprague-Dawley rats given a single oral dose of OSI-930 was incubated with β-glucuronidase at 37°C. The results of the incubation revealed a decrease in the area of the 552 *m/z* peak and the formation of a new peak with a molecular ion at 376 *m/z* and characteristic dTFM product ions, including an ion at 267 *m/z*, indicative of OSI-930. Incubation with glucuronidase produced a more lipophilic compound that is equivalent to the hydroxyl analogue without the trifluoromethyl, thus showing *O*-dealkylation of the trifluoromethyl or displacement of the trifluoromethoxy group (data not shown). The identity of this compound was confirmed by LC/MS/MS comparisons with the synthetic standard.

Intensity versus time data were collected from plasma at nominal times of 0.5, 1, 2, 4, 8, 12, 24, and 48 hours for three rats given a single oral 1000 mg/kg dose of OSI-930. Individual HPLC/MS peak area values and calculated median, minimum, and maximum values are shown for OSI-930 *des*-trifluoromethyl + glucuronide (552/267 *m/z*) and for dTMF (376/267 *m/z*). Median peak area values are shown in area versus time graphs in Figure 9. The largest median area values for both OSI-930 *des*-trifluoromethyl + glucuronide and dTFM occurred at the 12-hour time point. This is later than the median OSI-930 T_{max} value of 8 hours in the same dose group. The OSI-930 *des*-trifluoromethyl + glucuronide and dTFM curves roughly approximate each other over the time course of the experiment, with the median OSI-930 *des*-trifluoromethyl + glucuronide intensity being about 1000-fold greater than that of the dTFM metabolite. The intensity of the dTFM is comparatively too small to make any judgments about the T_{max} or any other kinetics of formation and clearance of the dTFM. Taken together, these two observations suggest that dTFM formation

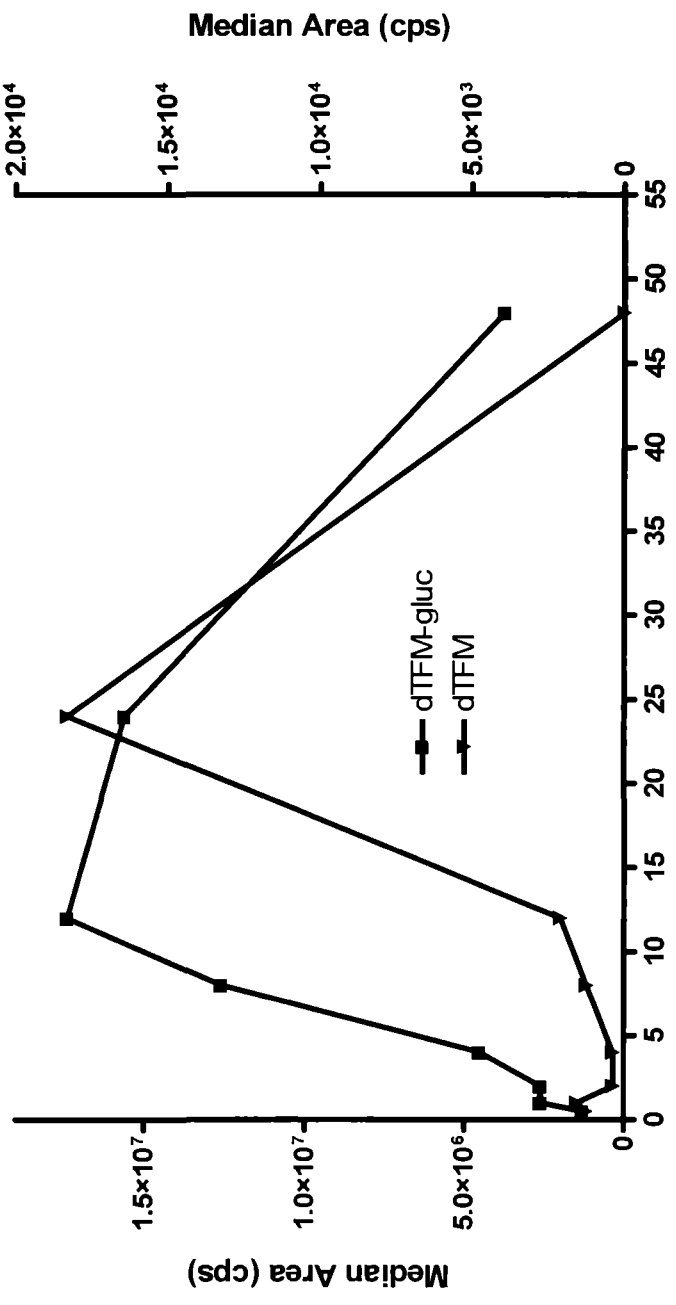

Fig. 9: OSI-930-*des*-trifluoromethyl + glucuronide (dTFM-gluc) and OSI-930-*des*-trifluoromethyl (dTFM) intensity versus time curves The y-axis is median area in counts per second (cps) and the x-axis is time in hours. (Zero was used as the input value for this graph instead of BLOQ for the 24-hour time point.)

is slow and likely the rate-limiting step leading to the formation of OSI-930 *des*-trifluoromethyl + glucuronide. The conjugation reaction is comparatively very efficient as the dTFM is usurped to the subsequent glucuronide which is about 1000x higher in concentration.

Incubations with rat and human hepatic microsomes also demonstrated the production of the dTFM. The MS spectrum also agreed with the standard. This observation reveals that the oxidative metabolism producing the dTFM can be performed with microsomal fraction constituents.

Since humans have been dosed with OSI-930 we were able to evaluate the circulating blood to determine whether the human species also systemically produces detectable amounts of the dTFM. Human plasma from Phase I patients, which also presents the dTFM metabolite product, demonstrated that the human liver enzyme produces sufficient quantities to be detectable systemically (data not shown).

We also determined the specific P450 isoform pathway responsible for catalyzing the trifluoromethoxy displacement by examining the product formation after *in vitro* incubations. Reaction product from selected P450 isoforms contained the dTFM from CYP3A4-mediated catalysis. A selection of P450 isoforms (CYP3A4, CYP2D6, CYP 2B6, and CYP2A6) from cloned cDNA expression systems were tested for the ability to produce the dTFM, with only CYP3A4 and to a negligible extent CYP2D6 catalyzing this biotransformation to the dTFM metabolite (Fig. 10). Thus the formation of the dTFM is CYP-mediated, and CYP3A4 is the major facilitator of this pathway with a detectable contribution by CYP2D6.

DISCUSSION

The observation described herein indicates the existence of a novel biotransformation beyond the already diverse set of atypical reactions that cytochrome P450 can catalyze /1,2/. To our knowledge, this is the first report of the CYP-mediated dealkylation of a trifluoromethoxy constituent *para* to an aminoacyl moiety.

This reaction is similar to the apparent *ipso* substitution at the *para* position of the aromatic ring of the trifluoromethoxy anisole moiety in CP-122,721 which was recently described /12/. Conventional *O*-dealkylation occurs via a hemiacetal intermediate produced by oxidation of the α-carbon of the ether /4/ as characterized in Figure 1.

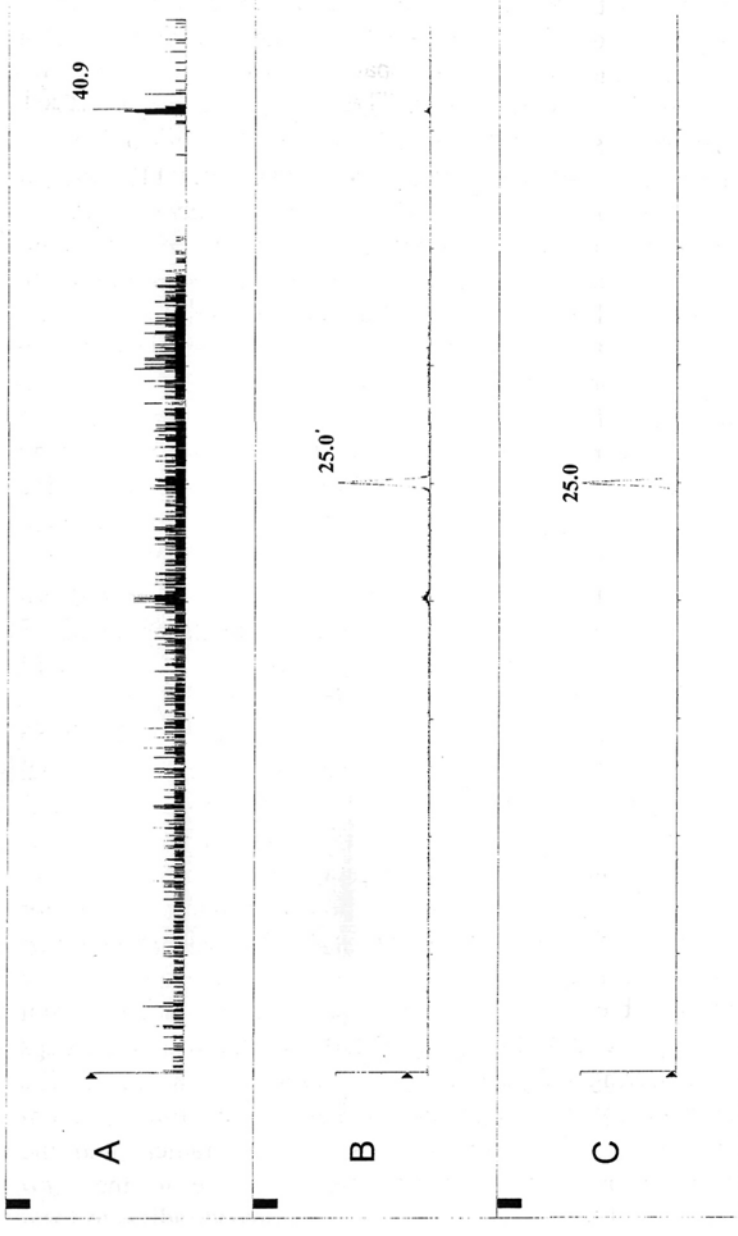

Fig. 10: **A:** OSI-930 incubated with recombinant CYP3A4 enzyme for zero time. **B:** OSI-930 incubated with recombinant CYP3A4 enzyme for 60 minutes. **C:** OSIP691251 only.

With the superior bond strength of the C-F bond over even the C-H bond, however, it is improbable that the trifluoromethoxy carbon is directly oxidized by the P450. Therefore, the *O*-detrifluoromethylation at this group was confounding which led to the consideration of a detrifluoromethoxylation via hydroxyl replacement and the conclusion that an *ipso* attack or radical mechanism appears operative. Consequently, we propose a CYP-mediated *ipso* substitution to displace the trifluoromethoxy group with a hydroxyl group (Fig. 11). Oxygen substitution at the phenyl radical and trifluromethoxy elimination produce the benzoquinone intermediate (similar to the phenacetin mechanism described below). Finally, benzoquinone reduction to the hydroquinone with glucuronidation produces the observed metabolite.

Certain halogenated benzenes demonstrate the essentials of *ipso* mechanism oxidation reactions. Following an electron and proton abstraction from 4-fluorinated anilines, the iron moiety donates a hydroxyl radical for recombination /13-15/. The unstable intermediate can lose a proton and fluoride anion to form the benzoquinoneimine (similar to Fig. 12a). Notably, the CF_3O^- moiety is very 'halogen-like' in terms of chemistry and electronegativity.

The *ipso*-substitution mechanism is not limited, however, to halogen-substituted phenols /13/. Type I *ipso* substitutions eliminate an anion from the quinol to *p*-benzoquinone, while type II substitutions eliminate a carbocation (hydroxylated with water) with hydroquinone as the intermediate /16/. The oxidative *O*-deethylation of phenacetin to paracetamol occurs through the formation of an unstable hemiketal at the α-methylene carbon atom, which decomposes rapidly /17/. Because phenacetin is also converted to the arylating metabolite *N*-acetyl-*p*-benzoquinone imine (NAPQI) that reacts with GSH /18/, however, this latter reaction provides a more important pathway for potential toxicity. Only about 50% of the oxygen in the phenolic group of the phenacetin conjugate came from ^{18}O-labeled molecular oxygen /19,20/. An unstable intermediate could convert to a geminal diol intermediate at position 4 of the ring, with one of the hydroxyl groups randomly lost during dehydration to the quinone-imine metabolite /19,20/. Alternatively, a hydrogen abstraction from the nitrogen atom in the acetylamino side chain yields a hydroxyl radical and the corresponding nitrogen radical which can rearrange to the *para* aromatic carbon and then recombine with the hydroxyl radical to form the hemiketal /21/. In the presence of a thiol (GSH), the sulfur

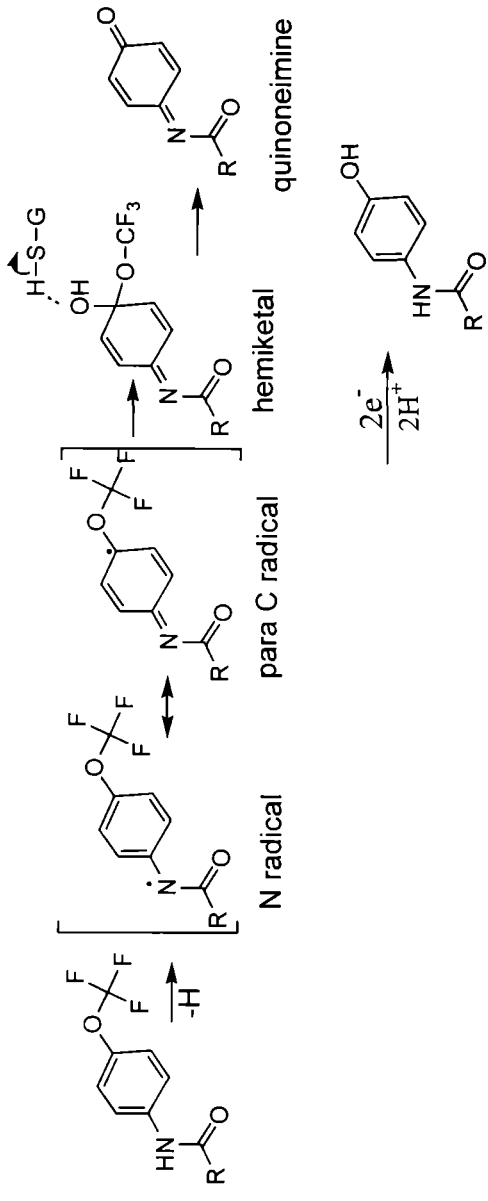

Fig. 11: Proposed *ipso* displacement of trifluoromethoxy.

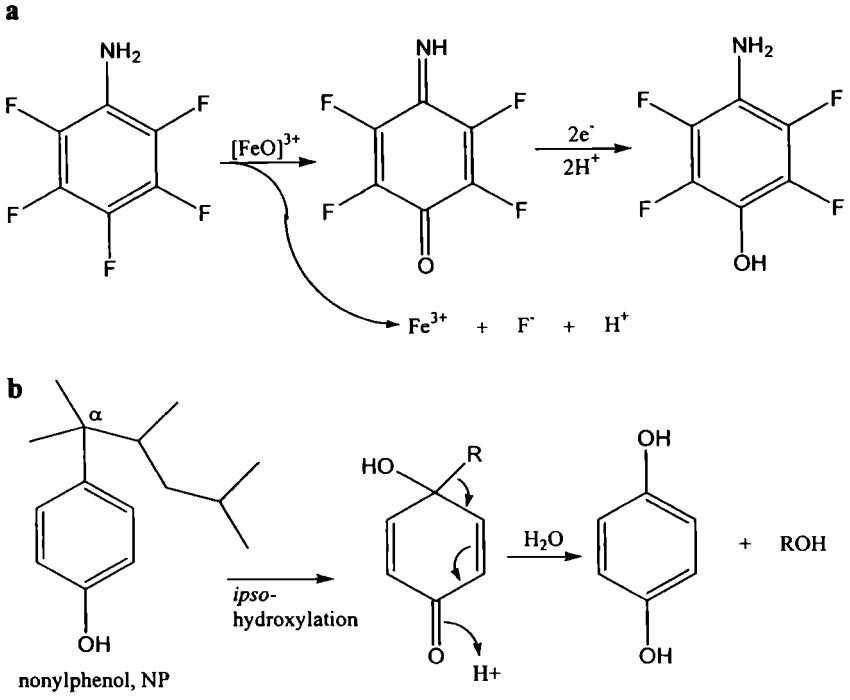

Fig. 12: **a:** Fluoroanaline dehalogenation by *ipso* mechanism. **b:** Nonlyphenol dealkylation by *ipso* mechanism

hydrogen may form a hydrogen bond with the hemiketal oxygen, while a coincident hydrogen bond between the hemiketal hydroxyl and the sulfur may also exist /21/, thus catalyzing quinone production with 100% incorporation of the activated oxygen. Conversely, a hydrogen bond between the sulfur and the hydroxyl can lead to 100% retention of the alkoxy oxygen. These possible alternate parallel pathways are consistent with the results showing about 50% incorporation of ^{18}O-labeled oxygen into the phenolic oxygen /19/.

Furthermore, product and kinetic analysis of hydrolysis reactions with several phenacetin analogues have indicated a nitrenium ion mechanism wherein oxygen is incorporated with coincident loss of the alkoxy of phenacetin /22/. P450-mediated reactions with aromatic substrates having N-H, O-H, C-H, or S-H substituents have been generalized to occur by this type of hydrogen abstraction, a delocalized radical to the center of substitution, and an iron-bound hydroxyl radical recombination mechanism /23/.

The P450-mediated conversion of pentahalogenated benzenes to quatra-halogenated phenols (Fig. 12a) has been demonstrated: the halogen atom *para* to the amino or hydroxyl moiety is released from the molecule as a halogen anion, resulting in a benzoquinone, which is then reduced to the corresponding aminophenol or hydroquinone /14/. The mechanism appears to involve formation of a benzohaloquinone with a positive charge on halogen substituents *para* to the dehalogenated position - stabilized through mesomeric structures. The pentahalogenated phenol is formed via a chemical two-electron reduction by NADPH. Monooxygenation at a fluorinated *para* position, such as in pentafluorophenol, results in the formation of the reactive tetrafluorobenzoquinone derivative as the primary reaction product /24/. P450-mediated halogen displacement is increasingly facile in the order I < Br < Cl < F, with additional electron-withdrawing halogen ring substituents further easing elimination /15/, despite the suggestion of fluorine substituents blocking drug biotransformation.

A comparable *ipso* substitution by the active oxygen species atom has been described with 4-(4-nitrophenoxy)phenol and other 4-hydroxyarylether analogues /8/. When there is a phenolic hydroxy *para* to the ether bond, a phenoxy radical via abstraction by the iron-oxenoid will delocalize and distribute to the *ipso* position, followed by recombination of the hydroxyl-radical equivalent on the heme iron to give a hemiketal /8/. Using $^{18}O_2$ along with various analogues with a requisite *para*-group /8/ also showed that cytochrome P450 could catalyze this *ipso*-substitution reaction. They further demonstrated significant elimination of the most electronegative halogen fluorine substituent attached to an aromatic ring /16/. Finally, of the many functional active oxidants in CYP-catalyzed reactions, the hydroperoxo-iron species is implicated as the electrophilic oxidant for *ipso* substitution of various *para*-substituted phenols via a transient intermediate involving the substituent *para* to the hydroxyl /25/. This study demonstrated P450-catalyzed hydroquinone formation from *t*-butylphenol by *ipso* substitution of the alkyl group /25/. In another molecular example (Fig. 12b), the hydroxylation at the C-4 position of the α-quaternary nonylphenol (to a hemiketal) leaves the alkylated quinol as a carbocation or radical species, producing hydroquinone via a type II *ipso* substitution mechanism in microbial degradation /26-28/. The *ipso*-hydroxy group from side-chain cleavage of an α-quaternary 4-nonylphenol was derived from molecular oxygen as

shown by ^{18}O-labeling experiments. The resulting nonanol metabolite contained an oxygen atom from water /29/. Our results and observations supplement the corroboration of an uncommon reaction that CYP catalysis can produce. Additionally, an *ipso* hydroxylation of the 8-prenylnaringenin B ring at a quaternary α-carbon site has been described /30/. Indeed, the bisphenol A degradation occurs via a type II *ipso*-substitution mechanism resulting in scission of the C-C bond between the phenolic moiety and the isopropyl group of bisphenol.

ACKNOWLEDGEMENTS

We are very grateful to Adriane L. Stewart for editorial assistance and to Arlindo Castelhano for review of the manuscript and mechanism schemes.

Source of financial support: OSI Pharmaceuticals, Inc.

REFERENCES

1. Guengerich FP. Uncommon P450-catalyzed reactions. Curr Drug Metab 2001; 2: 93-115.
2. Guengerich FP. Common and uncommon cytochrome P450 reactions related to metabolism and chemical toxicity Chem Res Toxicol 2001; 14: 611-650.
3. Al-Gailany KA, Bridges JW, Netter KJ. The dealkylation of some rho-nitrophenylalkylethers and their alpha-deuterated analogues by rat liver microsomes Biochem Pharmacol 1975; 24: 867-870.
4. Renson J, Weissbach H, Udenfriend S. On the mechanism of oxidative cleavage of aryl-alkyl ethers by liver microsomes. Mol Pharmacol 1965; 1: 145-148.
5. Miwa GT, Walsh JS, Lu AY. Kinetic isotope effects on cytochrome P-450 catalyzed oxidation reactions. The oxidative O-dealkylation of 7-ethoxycoumarin. J Biol Chem 1984; 259: 3000-3004.
6. Hecht SS, LaVoie EJ, Bedenko V, Pingaro L, Katayama S, Hoffmann D, Sardella DJ, Boger E, Lehr RE. Reduction of tumorigenicity and of dihydrodiol formation by fluorine substitution in the angular rings of dibenzo(αι)pyrene. Cancer Res 1981; 41: 4341-4345.
7. Park BK, Kitteringham NR. Effects of fluorine substitution on drug metabolism: pharmacological and toxicological implications. Drug Metab Rev 1994; 26: 605-643.
8. Ohe T, Mashino T, Hirobe M. Novel metabolic pathway of arylethers by cytochrome P450: cleavage of the oxygen-aromatic ring bond accompanying ipso-substitution by the oxygen atom of the active species in cytochrome P450 models and cytochrome P450. Arch Biochem Biophys 1994; 310: 402-409.

9. Park BK, Kitteringham NR, O'Neill PM. Metabolism of fluorine-containing drugs. Annu Rev Pharmacol Toxicol 2001; 41: 443-470.
10. Heidelberger C. The nucleotides of fluorinated pyrimidines and their biological activities. In: Elliot K, ed. Carbon-Fluorine Compounds: Chemistry, Biochemistry and Biological Activities. Amsterdam· Elsevier, 1972; 125-140.
11. Thompson DC, Perera K, London R. Spontaneous hydrolysis of 4-trifluoromethylphenol to a quinone methide and subsequent protein alkylation. Chem Biol Interact 2000; 126: 1-14.
12. Kamel A, Davis J, Potchoiba MJ, Prakash C. Metabolism, pharmacokinetics and excretion of a potent tachykinin NK1 receptor antagonist (CP-122,721) in rat: characterization of a novel oxidative pathway. Xenobiotica 2006; 36: 235-258.
13. Rietjens IM, Vervoort J. Bioactivation of 4-fluorinated anilines to benzoquinoneimines as primary reaction products. Chem Biol Interact 1991; 77: 263-281.
14 Rietjens IM, Vervoort J. A new hypothesis for the mechanism for cytochrome P-450 dependent aerobic conversion of hexahalogenated benzenes to pentahalogenated phenols. Chem Res Toxicol 1992; 5: 10-19.
15. Rietjens IM, den Besten C, Hanzlik RP, van Bladeren PJ. Cytochrome P450-catalyzed oxidation of halobenzene derivatives. Chem Res Toxicol 1997; 10: 629-635.
16. Ohe T, Mashino T, Hirobe M. Substituent elimination from p-substituted phenols by cytochrome P450. *ipso*-Substitution by the oxygen atom of the active species. Drug Metab Dispos 1997; 25: 116-122.
17. Garland WA, Nelson SD, Sasame HA. Primary and beta-secondary deuterium isotope effects in the O-deethylation of phenacetin. Biochem Biophys Res Commun 1976; 72: 539-545.
18. Nelson SD, Forte AJ, Vaishnav Y, Mitchell JR, Gillette JR, Hinson JA. The formation of arylating and alkylating metabolites of phenacetin in hamsters and hamster liver microsomes. Mol Pharmacol 1981; 19: 140-145.
19. Hinson JA, Nelson SD, Mitchell JR. Studies on the microsomal formation of arylating metabolites of acetaminophen and phenacetin. Mol Pharmacol 1977; 13: 625-633.
20. Hinson JA, Nelson SD, Gillette JR. Metabolism of [p-18O]-phenacetin: the mechanism of activation of phenacetin to reactive metabolites in hamsters. Mol Pharmacol 1970; 15: 419-427.
21. Koymans L, Van Lenthe JH, Donne-op Den Kelder GM, Vermeulen NP. Mechanisms of activation of phenacetin to reactive metabolites by cytochrome P-450: a theoretical study involving radical intermediates. Mol Pharmacol 1990; 37: 452-460.
22. Novak M, Pelecanou M, Zemis JN. Detection of N-acetyl-p-benzoquinone imine produced during the hydrolysis of the model phenacetin metabolite N-(pivaloyloxy)phenacetin. J Med Chem 1986; 29: 1424-1429.
23. Koymans L, Donne-Op den Kelder GM, te Koppele JM, Vermeulen NP Generalized cytochrome P450-mediated oxidation and oxygenation reactions in

aromatic substrates with activated N-H, O-H, C-H, or S-H substituents. Xenobiotica 1993; 23: 633-648.
24. den Besten C, van Bladeren PJ, Duizer E, Vervoort J, Rietjens IM. Cytochrome P450-mediated oxidation of pentafluorophenol to tetrafluorobenzoquinone as the primary reaction product. Chem Res Toxicol 1993; 6: 674-680.
25. Vatsis KP, Coon MJ. Ipso-substitution by cytochrome P450 with conversion of p-hydroxybenzene derivatives to hydroquinone: evidence for hydroperoxo-iron as the active oxygen species. Arch Biochem Biophys 2002; 397: 119-129.
26. Gabriel FL, Heidlberger A, Rentsch D, Giger W, Guenther K. Kohler HP. A novel metabolic pathway for degradation of 4-nonylphenol environmental contaminants by *Sphingomonas xenophaga* Bayram: ipso-hydroxylation and intramolecular rearrangement. J Biol Chem 2005; 280: 15526-15533.
27. Corvini PF, Hollender J, Ji R, Schumacher S, Prell J, Hommes G, Priefer U, Vinken R, Schäffer A. The degradation of alpha-quaternary nonylphenol isomers by *Sphingomonas* sp. strain TTNP3 involves a type II ipso-substitution mechanism. Appl Microbiol Biotechnol 2006; 70: 114-122.
28. Kolvenbach B, Schlaich N, Raoui Z, Prell J, Zühlke S, Schäffer A, Guengerich FP, Corvini PF. Degradation pathway of bisphenol A: does ipso substitution apply to phenols containing a quaternary alpha-carbon structure in the para position? Appl Environ Microbiol 2007; 73: 4776-4784.
29. Gabriel FL, Cyris M, Jonkers N, Giger W, Guenther K, Kohler HP. Elucidation of the ipso-substitution mechanism for side-chain cleavage of alpha-quaternary 4-nonylphenols and 4-t-butoxyphenol in *Sphingobium xenophagum* Bayram. Appl Environ Microbiol 2007; 73: 3320-3326.
30. Nikolic D, Li Y, Chadwick LR, Grubjesic S, Schwab P, Metz P, van Breemen RB. Metabolism of 8-prenylnaringenin, a potent phytoestrogen from hops (*Humulus lupulus*), by human liver microsomes. Drug Metab Dispos 2004; 32: 272-279.